LBL-27767
UC-814

Lawrence Berkeley Laboratory
UNIVERSITY OF CALIFORNIA

EARTH SCIENCES DIVISION

Prediction of Release Rates for a Potential Waste Repository at Yucca Mountain

M.M. Sadeghi, T.H. Pigford, P.L. Chambré, and W.W.-L. Lee

October 1990

Prepared for the U.S. Department of Energy under Contract Number DE-AC03-76SF00098

DISCLAIMER

LBL-27767
UC-814

Prediction of Release Rates for a Potential Waste Repository at Yucca Mountain

M. M. Sadeghi, T. H. Pigford, P. L. Chambré, and W. W.-L. Lee

Department of Nuclear Engineering
University of California

and

Earth Sciences Division
Lawrence Berkeley Laboratory
University of California
Berkeley, California 94720

October 1990

This work was supported in part by the Director, Office of Civilian Radioactive Waste Management, Office of Systems Integration and Regulations, Licensing and Compliance Division, and by the Yucca Mountain Project Office, of the U.S. Department of Energy under Contract No. DE-AC03-76SF00098.

The authors invite comments and would appreciate being notified of any errors in the report.

T. H. Pigford
Department of Nuclear Engineering
University of California
Berkeley, CA 94720

CONTENTS

1. INTRODUCTION 1
2. WATER-CONTACT MODES 1
2.1 The Wet-Drip Water Contact Mode 1
2.2 The Moist-Continuous Water-Contact Mode 2
3. PARAMETERS ADOPTED FOR CALCULATING RELEASE RATES 2
3.1 Waste Package 2
3.2 Hydrogeologic Conditions 3
Hydrologic Conditions 3
Diffusion Coefficient 4
3.3 Reaction Parameters 4
Matrix Alteration Rates 4
Solubility 4
Sorption Ratios 8
3.4 Data for Release Modes 8
4. CALCULATED RELEASE RATES 9
4.1 Wet-Drip Bathtub Water Contact Release Rates 9
4.1.1 Solubility-Limited Species 10
4.1.2 Alteration-Controlled and Instant-Release Species 11
4.2 Moist-Continuous Water-Contact Release Rates 12
4.2.1 Solubility-Limited Release into Tuff Directly 12
4.2.2 Solubility-Limited Release Through a Rubble-Filled Annulus 12
4.2.3 Alteration-Controlled Release Through a Rubble-Filled Annulus 14
5. CONCLUSIONS AND RECOMMENDATIONS 15
REFERENCES 16

FIGURES

Fig. 1. The alteration of UO_2 5

Fig. 2. Fractional release rates of plutonium isotopes, wet-drip bathtub, water contact at 1000 years, water inflitration rate 0.5 mm/a 19

Fig. 3. Fractional release rates of americium isotopes, wet-drip bathtub, water contact at 1000 years, water inflitration rate 0.5 mm/a 20

Fig. 4. Fractional release rates of neptunium and uranium isotopes, wet-drip bathtub, water contact at 1000 years, water inflitration rate 0.5 mm/a 21

Fig. 5. Fractional release rates of U-234→Th-230→Ra-226 chain, wet-drip bathtub, water contact at 1000 years, water inflitration rate 0.5 mm/a 22

Fig. 6. Fractional release rates of alteration-controlled species and their instant release fractions, wet-drip bathtub, water contact at 1000 years, water inflitration rate 0.5 mm/a 23

Fig. 7. Fractional release rates of americium, neptunium and uranium isotopes directly into intact tuff, moist-continuous water contact 24

Fig. 8. Fractional release rates of plutonium isotopes directly into intact tuff, moist-continuous water contact 25

Fig. 9. Fractional release rates of plutonium isotopes through a rubble-filled annulus into intact tuff, moist-continuous water contact, with 1000-fold reduction of diffusion coefficient in annulus 26

Fig. 10. Fractional release rates of americium isotopes through a rubble-filled annulus into intact tuff, moist-continuous water contact, with 1000-fold reduction of diffusion coefficient 27
28

Fig. 11. Fractional release rates of alteration-controlled species, through a rubble-filled annulus into intact tuff, moist-continuous water contact, with 1000-fold reduction of diffusion coefficient in annulus . . . 28

1. INTRODUCTION

Nuclear waste may be placed in the potential repository at Yucca Mountain in waste packages. The waste will consist of spent fuel assemblies or consolidated fuel rods, as well as borosilicate glass in steel pour containers, each enclosed in sealed containers. Current design calls for the waste packages to be surrounded by an air gap. Although the waste package is generally not seen as the primary barrier for nuclear waste isolation, it must in fact meet specific regulatory requirements. In 10 CFR 60.113(a)(1)(ii)(B), the U. S. Nuclear Regulatory Commission requires that the release rate of any radionuclide from the engineered barrier system following the containment period shall not exceed one part in 100,000 per year of the inventory of that radionuclide calculated to be present at 1,000 years following permanent closure. For low-inventory radionuclides, those that constitute less than 0.1 percent of the calculated total curie inventory at 1,000 years, the allowable annual release is a constant value, equal to 10^{-8} of the total curie inventory in the repository at 1,000 years. Therefore it is necessary to calculate release rates for waste packages at Yucca Mountain.

In this report, we calculate release rates for key radionuclides using analytic solutions presented in a companion report.[1] We consider both wet-drip and moist-continuous water-contact modes. This work is an expansion of previous results.[2]

We consider the release of three types of species: solubility-limited species, species released congruent with solid-solid alteration of spent-fuel matrix or borosilicate glass, and readily soluble species from the fuel-cladding gap, gas plenum, and readily accessible grain boundaries. In each case we give the release rates of the species as a function of time.

2. WATER-CONTACT MODES

We consider two modes of water contact that lead to the release of radionuclides.

2.1 The Wet-Drip Water Contact Mode

First we consider the dripping of water from overhead rock onto waste packages. This dripping may happen because of episodic fracture flow or a change in rock permeability may divert water into fractures that intersect the borehole. Drips are assumed to penetrate cracks in a failed container and to dissolve radionuclides as the radionuclide solution slowly rises in the container and finally overflows through other cracks and penetrations. Overflow of contaminated water is assumed to occur only near the top of the container. The contaminated water drips to the rock below. Water within the container is always well mixed from diffusion and thermal convection. We refer to this as the "wet-drip bathtub water-contact mode."

2.2 The Moist-Continuous Water-Contact Mode

The wet-drip mode assumes that the waste container and air-filled annulus surrounding a waste package preclude pathways for diffusive release of dissolved species. However, there can exist pathways for release by liquid diffusion if a failed waste package contacts the surrounding rock by physical displacement, if the annulus becomes filled with sediments and rubble, or if the surrounding rock becomes water saturated.[2] For this report we assume rubble in the annulus has the same moisture content as the surrounding rock.

We assume that water has filled a failed container, and we neglect mass-transfer resistance from Zircaloy fuel cladding and from the residual container material and corrosion products. For the expected ground-water velocities, and for the diffusion coefficients assumed here for intact rock, mass-transfer is predicted to occur predominantly by molecular diffusion in pore liquid in the rock matrix.[3] Under these conditions the release rate is finite at zero velocity and is insensitive to any but very large increases in water velocity.

We conservatively assume that all moisture in the intact rock is in interconnected water-filled pores, with a pore-liquid diffusion coefficient given by that for a liquid continuum. As a result of the low effective diffusion coefficient for unsaturated rubble, with air in void spaces not occupied by rubble, the predicted mass transfer rates will be far below what could occur if the repository were saturated or if the degraded waste container were in close contact with consolidated or intact rock. Our analyses will be restricted to the unsaturated environment, so this particular type of contact is more aptly termed the "moist-continuous water-contact mode," and is so referred to herein.

3. PARAMETERS ADOPTED FOR CALCULATING RELEASE RATES

3.1 Waste Package

Table I lists the dimensions of a defense waste container. The diameter and height of borosilicate pour canister are 0.61 m and 3 m respectively and those of the outside container are 0.66 m and 3.28 m respectively. The expected fill volume is 85 percent of pour canister capacity. The internal void volume in the container is 0.42 m^3.

For spent fuel we consider a reference container with three PWR assemblies, Table II. The initial uranium inventory in this package is 1.5 Mg. The void volume inside this waste container is estimated to be 1.5 m^3, obtained after we subtract the volume of fuel rods (0.14 m^3) and the volume of fuel dividers (0.015 m^3) from the container volume (1.63 m^3). The volume due to fuel-cladding gap has been neglected. To obtain the radius of an equivalent-area spherical waste package, we compute the surface area of the cylindrical waste container, set it equal to that of a sphere, and solve for the sphere radius.

Table I. Defense Waste Container Characteristics

Diameter of pour canister (m)	0.61
Diameter of container (m)	0.66
Overal cross-sectional area (m^2)	0.34
Cross-sectional area of waste glass (m^2)	0.27
Internal void volume (m^3)	0.42
Radius of equal-area sphere (m)	0.74
Height of pour canister (m)	3.0
Height of outside container (m)	3.28

Source: Ref. 4 and 5

Table II. Spent Fuel Container Characteristics

Number of PWR assemblies per waste container	3
Uranium inventory, initial (Mg)	1.5
Container height (m)	4.76
Container diameter (m)	0.66
Cross-sectional area (m^2)	0.34
Internal void volume (m^3)	1.5
Average diameter of fuel rods (cm)	1
Average length of fuel rods (m)	3.33
Number of fuel rods per assembly	182
Fuel dividers thickness (cm)	0.32
Radius of equal-area sphere (m)	0.92

Source: Ref. 4 and 5.

3.2 Hydrogeologic Conditions

Hydrologic Conditions

The far-field averaged flux at the emplacement horizon is taken to be 0.5 mm/a, which appears to be an upper bound for expected conditions.[5,6] For a container cross-sectional area of 0.34 m^2, we calculate a volumetric flow rate into the container by multiplying the flux of water and the cross-sectional area, or 1.71×10^{-4} m^3/a. We use this volumetric flow into failed containers in the wet-drip bathtub water-contact mode.

Diffusion Coefficient

The diffusion coefficient has been determined experimentally for cesium in moisture present in intact tuff, and the value is 3×10^{-6} cm^2/s.[7] This value includes a tortuosity reduction. For an unconsolidated rubble bed of partially saturated porous media, we must include additional tortuosity effects due to the tortuosity of the contact areas between rubble particles. To illustrate, we adopt a 1000-fold reduction in the diffusion coefficient for the rubble bed.[8]

3.3 Reaction Parameters

Matrix Alteration Rates

The matrix of spent fuel is mostly UO_2. The oxidative reactions of UO_2 have been studied extensively in the laboratory.[9,10] The first reaction is the surface oxidation of UO_2 to UO_{2+x}, $x < 0.33$, which is limited to a few monolayers of the surface. The reaction

$$3UO_2 + H_2O \Longleftrightarrow U_3O_7 + 2H^+ + 2\,e^-$$

forms a protective layer of U_3O_7 of up to 4 nm thickness. If the redox conditions promotes further oxidation, at an Eh of about +100 mV, then the reaction has been postulated

$$U_3O_7 \text{ (fluorite)} \rightarrow U_2O_5 \rightarrow U_3O_8 \text{(orthorhombic)}$$

to take place and a major crystallographic rearrangement occurs. The structural change releases fission products and actinides for reaction with the water. The overall reaction scheme for UO_2 in oxygenated waters is depicted in Figure 1. There is experimental evidence that the reaction rates are highly dependent on the redox conditions.[11]

We use an experimental rate of alteration of UO_2 determined in spent-fuel leaching experiments. Wilson measured the concentration of various species from spent fuel segments, leached in J-13 water in hot cells.[12] The best estimate of the alteration rate appears to be 1×10^{-3}/a.

There is an equivalent alteration of borosilicate glass in the presence of water, releasing fission products and actinides. From the experimental dissolution rate of lithium from borosilicate glass,[13] the rate of reaction of the SiO_2 glass matrix with water is 5.2 g/m^2-a. For a container with 1660 kg glass and assuming that the total reaction surface area, due to internal cracks, is 25 times the geometrical surface area (0.27 m^2),[4,15] the reaction rate would become 36 g/a. This results in a fractional alteration rate of 2×10^{-5}/a.

Solubility

The alteration of spent fuel or glass results in precipitates of actinides on the waste-form surface. For calculating the release rates of these solubility-limited species, the elemental solubility is needed. For solubilities

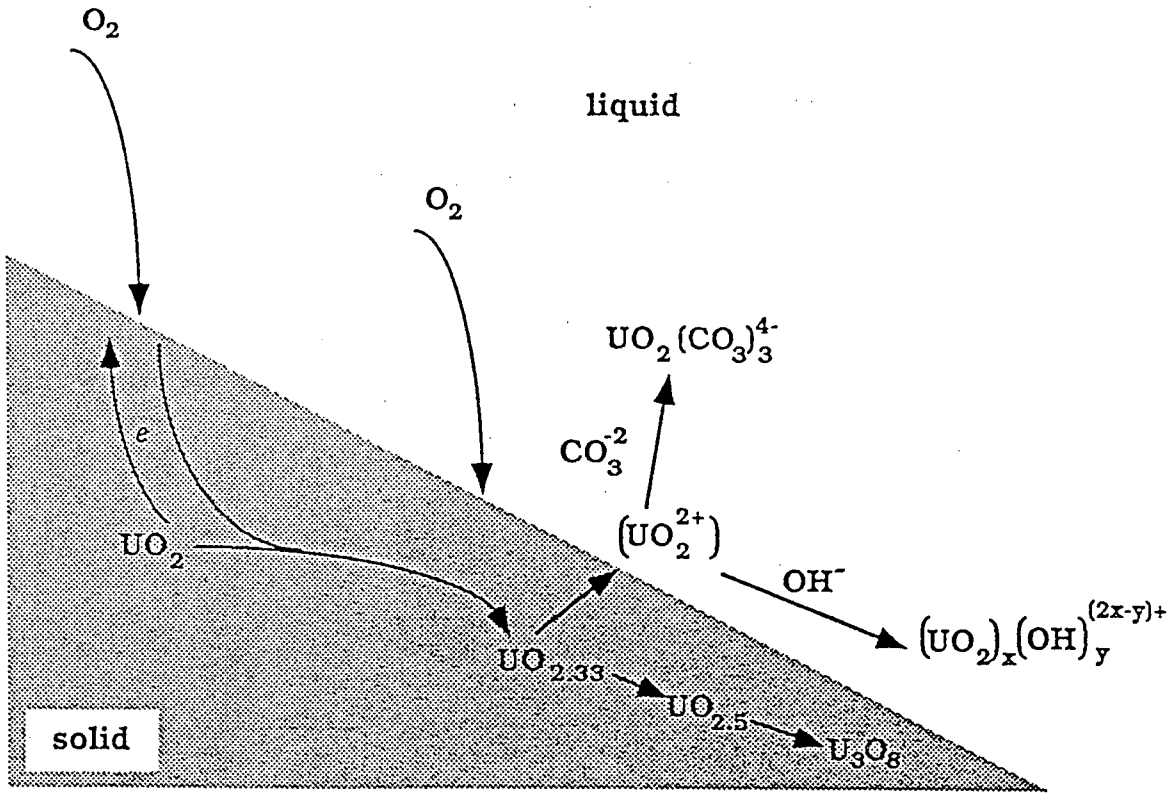

Figure 1. Reaction Scheme for UO_2 in Oxidizing Water, Adapted from Johnson & Shoesmith[11]

of U, Np, Pu and Am dissolving from spent fuel, we use the concentrations of these elements measured in hot-cell leaching experiments of decladded spent fuel,[14,12] shown in Table III.

Solubilities of U, Np, Pu and Am dissolving from borosilicate glass have been calculated using the geochemical code EQ3/6 to simulate hot-cell leaching experiments of Wilson.[15] The geochemical simulations sought to reproduce experimental results and show which solid species are controlling the solubility. The simulation shows the mass of various species in solution versus reaction progress, as well as the identity of the controlling solid phases. There are problems and uncertainties associated with obtaining solubilities this way, because of database limitations, uncertainties in the interpretation of measured steady-state radionuclide concentrations, and uncertainties in the determination of what precipitates that will form to control solute concentrations.

According to a geochemical simulation of uranium release from the reaction of spent fuel with J-13 water at 25°C,[16] uranium concentration in solution is related to the concentration of SiO_2 in solution. When the reaction first begins, the uranium concentration increases until saturation of hawiweeite ($Ca(UO_2)_2Si_6O_{15}\cdot 5H_2O$). The concentration of uranium is then maintained at 0.04 mg/kg. Soddyite ($(UO_2)_2SiO_2\cdot 2H_2O$) later precipitates, increasing the concentration of uranium to 0.1 mg/kg. After depletion of silica in solution by precipitation of these uranyl silicates, the uranium concentration increases to 87 mg/kg. Precipitation of schoepite ($UO_3\cdot 2H_2O$) then reduces uranium concentration slightly, at 100 g of glass reacted per kg of water, the end of the simulation. Through this simulation of the dissolution of 100 g of glass, the concentration of

uranium varied over five orders of magnitude. From that variation we select a single uranium solubility to use in the calculations, at 100 g of glass reacted per kg of water reacted.

The solubilities of uranium, plutonium, americium and neptunium in borosilicate glass, shown in Table IV, have been obtained from geochemical simulation.[15] We use the solubilities of these species when precipitation first occurs.

There are large uncertainties in the solubilities used in these calculations. To illustrate the problem of calculating solubilities from a geochemical code, we compare in Table V Nitsche's[17] measured solubilities for americium, neptunium, and plutonium and the calculated solubilities of each of these elements in J-13 water at 25°C and *p*H 7. To measure the solubility of individual actinides at various temperatures and *p*H soluble actinide is added until a precipitate is formed and an equilibrium or steady-state concentration is reached. Ideally the composition of the precipitate is experimentally determined and equilibrium constants measured. When EQ3/6 predicts the same solid phase to be controlling the solubility, as in the case of americium, the experimental value agrees with the calculated value. For plutonium and neptunium, the large discrepancies between the experimental and calculated solubilities are attributed to the incorrect solid phase assumed for the calculation. The data base for EQ3/6 does not contain solubility-product constants for the solid phases identified in Nitsche's experiments. Thus, for reliable geochemical simulations using EQ3/6 the solid-phase data base must be extended.

Comparing the experimental solubilities for the pure actinides in Table V with the experimental solubilities for actinides from spent fuel in Table III, each pure-actinide solubility is greater than that for the same element from spent fuel. For neptunium the difference is about five orders of magnitude. The differences are explained on the grounds that the solid phases formed in spent-fuel dissolution are not the same as those formed in Nitsche's experiments with the individual actinides. Evidently the solid phases resulting in the mixed system from spent fuel are much less soluble.

The predicted solubilities for actinides from borosilicate glass are in some instances less and in other instances greater than those predicted for individual actinides. Here the solubilities are apparently predicted from the same data base in EQ3/6. Evidently the differences are due to the different solid phases that are predicted to result in the dissolution of borosilicate glass. The validity of the predicted solubilities for actinides from borosilicate glass must be questioned because of the differences between the calculated and experimental solubilities in Table V.

There remains much uncertainty in what solubilities are most appropriate for release-rate calculations. Validation of solubilities is of prime importance for reliable predictions of release rates. For most of the actinides, considerable uncertainty can be tolerated when the predicted release rates are far below those that would exceed a regulatory limit.

Table III. Solubility and Inventory Data for the Reference Spent-Fuel Package

Species	Half Life	Elemental Solubility		1000-a inventory
	(years)	(g/m^3)	Source	(g/pkg)
Tc-99	2.15×10^6	1.0×10^4	Ref. 18	1.15×10^3
I-129	1.59×10^7	not used	-	2.67×10^2
Cs-135	2.0×10^6	6.3×10^{-1}	Ref. 19	4.50×10^2
Ra-226	1.60×10^3	6.8×10^{-2}	Ref. 5	4.7×10^{-3}
Th-230	7.7×10^3	2.3×10^{-4}	Ref. 5	1.35
Np-237	2.16×10^6	3.0×10^{-4}	Ref. 14	2.1×10^3
Pu-239	2.41×10^4	9.5×10^{-4}	Ref. 14	7.3×10^3
Pu-240	6.54×10^3	9.5×10^{-4}	Ref. 14	3.1×10^3
Pu-242	3.8×10^5	9.5×10^{-4}	Ref. 14	6.75×10^2
U-234	2.44×10^5	0.3	Ref. 14	4.88×10^2
U-238	4.47×10^3	0.3	Ref. 14	1.4×10^6
Am-241	4.32×10^2	3.8×10^{-5}	Ref. 14	3.90×10^2
Am-243	7.37×10^3	3.8×10^{-5}	Ref. 14	1.3×10^2

Table IV. Solubility and Inventory Data for the Reference Defense-Waste Package

Species	Half Life	Elemental Solubility		1000-a inventory
	(years)	(g/m^3)	Source	(g/pkg)
Tc-99	2.15×10^6	1.0×10^4	Ref. 18	1.65×10^2
I-129	1.59×10^7	not used	-	0
Cs-135	2.0×10^6	6.3×10^{-1}	Ref. 19	1.02×10^2
Ra-226	1.60×10^3	6.8×10^{-2}	Ref. 5	5.14×10^1
Th-230	7.7×10^3	2.3×10^{-4}	Ref. 5	7.4×10^3
Np-237	2.16×10^6	9.4×10^{-2}	Ref. 15	1.59×10^1
Pu-239	2.41×10^4	3.8×10^{-8}	Ref. 15	4.18×10^1
Pu-240	6.54×10^3	3.8×10^{-8}	Ref. 15	7.0
Pu-242	3.8×10^5	3.8×10^{-8}	Ref. 15	6.3×10^{-1}
U-234	2.44×10^5	6×10^{-2}	Ref. 15	1.4×10^1
U-238	4.47×10^3	6×10^{-2}	Ref. 15	2.4×10^4
Am-241	4.32×10^2	1.5×10^{-3}	Ref. 15	3.7
Am-243	7.37×10^3	1.5×10^{-3}	Ref. 15	3.3×10^{-1}

Sorption Ratios

Retardation coefficients used in the moist-continuous calculations are obtained from experimental sorption ratios (Table VI) in the *Site Characterization Plan.*[5] The sortion coefficients are averaged values of tuff samples YM-22, GU3-1203, G1-1292, GU3-1301, YM-30, and JA-18. All these samples are in the Topopah Spring member of the Paintbrush tuff, the potential repository horizon. To calculate the retardation coefficient, a porosity of 0.16 and a bulk density of 2.5 g/cm^3 have been used. Table VII shows the wells and the depth of these samples. The locations of the wells are shown in the *Site Characterization Plan.*

Table V. Experimental and Calculated Solubilities According to Nitsche[17]

	Measured in J-13 Water 25°C and *p*H=7	Calculated for J-13 Water 25°C and *p*H=7
Np	1.1×10^{-4} moles/L 26.1 g/m^3	8×10^{-7} moles/L 0.19 g/m^3
solid	$NaNpO_2CO_3 \cdot 2.5H_2O$	NpO_2
Pu	3×10^{-7} moles/L 0.07 g/m^3	5×10^{-13} moles/L 1.2×10^{-7} g/m^3
solid	polymer & CO_3	PuO_2
Am	1.1×10^{-9} moles/L 2.7×10^{-4} g/m^3	6×10^{-9} moles/L 1.5×10^{-3} g/m^3
solid	$Am(OH)CO_3$	$Am(OH)CO_3$

Table VII. Data Source for Sorption Ratios[5]

Tuff Sample	From Well	Depth (m)
G1-1292	USW G-1	393.7
GU3-1203	USW GU-3	366.6
GU3-1301	USW GU-3	396.4
JA-18	J-13	432.7
YM-22	UE25a#1	258.4
YM-30	UE25a#1	385.1

3.4 Data for Release Modes

Tables VIII and IX list data relevant to the water contact modes. For releases of readily soluble nuclides from spent fuel, we assume two percent of the inventory of the respective species is available for instant dissolution, a reasonable value for light water reactor fuels.[6]

Table VI. Data for sorption ratios

	Sorption ratio (ml/g)[5]	Retardation coefficient
Technetium	0.16	3.4
Iodine	0	1
Cesium	417	6360
Uranium	1.8	28
Neptunium	4.9	76
Plutonium	208	3180
Americium	1070	16300

Table VIII. Data for Wet-Drip Water-Contact Mode

	Spent fuel	Borosilicate glass
Assumed Darcy velocity[5] (mm/yr)	0.5	0.5
Volumetric flow rate (m^3/yr)	1.71×10^{-4}	1.71×10^{-4}
Void volume[4,5] (m^3)	1.5	0.42
Fractional alteration rate[12,14] (1/yr)	0.001	2×10^{-5}

4. CALCULATED RELEASE RATES

In this section we show calculated release rates for selected radionuclides from spent-fuel and borosilicate glass waste packages. In all cases fractional release rates have been calculated at the edge of the engineered barrier system, defined here to be the inner surface of the emplacement borehole. The results are organized by the water-contact mode and the type of release mechanism. In each case we calculate release rates for a single waste package. A repository-ensemble release rate can be obtained by convolution with the time-distributed water-contact time,[20] or by conservatively assuming that the single waste package is indicative of the entire repository.

4.1 Wet-Drip-Bathtub Water-Contact Release Rates

For wet-drip water contact modes, we assume that water contact begins at 1000 years. For the spent-fuel container with an internal void space of 1.5 m^3, it takes about 8600 years to fill the container, and overflow first occurs at 9600 years. At this time the release of the species begins. For the borosilicate-glass container, the internal void volume is 0.42 m^3, and overflow begins at 3400 years. For all wet-drip release rates, the release rates are shown to 100,000 years.

Table IX. Data for Wet-Continuous Water-Contact Mode

	Spent fuel	Borosilicate glass
Radius of equivalent spherical waste package[4,5] (m)	0.92	0.74
Porosity of intact rock[5]	0.16	0.16
Rubble-bed porosity[6] (volume of air between rubble pieces ÷ total annulus volume)	0.30	0.30
Saturation fraction in the rubble[6]	0.86	0.86
Saturation fraction in the rock[6]	0.86	0.86
Assumed diffusion coefficient in intact rock[5] (m^2/yr)	9.5×10^{-3}	9.5×10^{-3}
Fractional alteration rate[12,14] (1/yr)	0.001	2×10^{-5}
Annulus thickness[6] (m)	0.03	0.03
Void volume[4,5] (m^3)	1.5	0.42
Container surface area (m^2)	10.6	6.9

4.1.1 Solubility-Limited Species

Most of the actinides in nuclear waste are likely to be solubility-limited in their release rates. Eq. (7) in Sadeghi *et al.*[1] is used to compute the wet-drip solubility-limited release rate. Figure 2 shows the release rates of plutonium species, normalized to the 1000-year inventories. Release begins at 9600 years for a spent-fuel container. The release rates at 9600 years reflect the distribution of the isotopes of plutonium at that time. As the 6540-year Pu-240 decays, the inventory is shared among the remaining isotopes, Pu-239 and Pu-242. This increases the release rate of Pu-239 until about 60,000 years when its own decay is sufficient to cause the release rate to decrease. The release rate of Pu-242, the longest-lived isotope, always increases as long as plutonium is solubility limited. The pattern is similar for release from borosilicate glass. The lower release rate from borosilicate glass is due to the lower solubility of plutonium. In all cases the release rates are very low.

Figure 3 shows the normalized release rates of americium species. Here there are only two isotopes, Am-241 and Am-243. The contribution of Am-241 to the release rate of spent fuel fades rapidly due to its short half life of 432 years. In borosilicate glass the relative contribution from Am-241 is greater. Due to the high solubility used for americium in glass, the fractional release rate of Am-243 is close to 1×10^{-5}/a.

Figure 4 shows the normalized release rates of neptunium and uranium isotopes. After release in the wet-drip mode begins, the Np-237 release rate continues unchanged for the time period shown in this figure, because

of the long half life. The normalized release rate for Np-237 is greater for glass than for spent fuel because of the lower inventory of Np-237 in glass. U-238 behaves like Np-237, with a constant release rate once release starts. Decay begins to decrease the release rate of U-234 at around 40,000 years. The differences of uranium release rates from spent fuel and glass result from the combined effect of different solubilities and inventories.

Figure 5 shows the release rates of the U-234→Th-230→Ra-226 chain from spent fuel and borosilicate glass. The release rate of U-234 is limited by its elemental solubility, and the releases of the daughters Th-230 and Ra-226 are assumed to be congruent with U-234. Eqs. (9), (16) and (22) in Sadeghi *et al.*[1] are used to compute these release rates. In the release of U-234 from spent fuel, U-234 release rate shows a slow decrease due to decay. The normalized release rates of Th-230 and Ra-226, however, show large increases due to rising inventories from precursor decay. In the reference defense waste Th-230 is initially near secular equilibrium with U-234, so the normalized release rate of Th-230 decreases with time. The fractional release rate of every member of the chain U-234→Th-230→Ra-226 is low, compared with the USNRC guideline.

4.1.2 Alteration-Controlled and Instant-Release Species

In spent fuel the soluble cesium, iodine, and technetium that exist in fuel-cladding gap, fuel plenum, and grain boundaries are treated as the instant-release or instant-dissolution fractions. Upon contact with water, the instant-dissolution fractions of these species are assumed to dissolve rapidly. In the wet-drip water-contact mode, the instantly released fraction stays in the water accumulating in the partly failed container until overflow. In the time between first water contact and overflow, another mechanism may become a more important mass transfer mechanism. For some of the highly soluble species in the waste matrix, laboratory studies suggest that their release may be congruent with the alteration of the waste matrix when it reacts with water, such as conversion of UO_2 in spent fuel to U_3O_8 and the conversion of silica in borosilicate glass to a crystalline mineral phase. In spent fuel the instant-release fraction is assumed to rapidly dissolve when water first contacts the waste. As the water level rises in the partly failed container, alteration of the UO_2 matrix proceeds. At overflow it would be impossible to distinguish the result of the two processes. We can, however, attribute part of the release to the instant-release fraction and the remainder to matrix alteration.

Figure 6 shows the normalized release of Tc-99, I-129 and Cs-135 from spent fuel and Tc-99 and Cs-135 from borosilicate glass. Equations for these calculations are given in Section 3.3 of Sadeghi *et al.*[1] The spent fuel alteration rate used is 1×10^{-3} per year of the original inventory, and the glass alteration rate is 2×10^{-5} per year. For spent fuel, the instant release fraction is set at two percent of the inventories of the species. Much of the alteration of spent fuel is completed while the failed container fills. The slower alteration rates of glass result in continued increase in concentration and release rate of the soluble species, followed by rapid decrease at the end of the alteration period.

4.2 Moist-Continuous Water-Contact Release Rates

Pathways for release by liquid diffusion may exist if a waste package contacts the surrounding rock by physical displacement, if the annulus becomes filled with sediments and rubble, or if the surrounding rock becomes water-saturated. We first calculate the rate of release directly from the failed waste container into the surrounding tuff, then we calculate the rate of release from a failed container into a rubble-filled annulus and thence into intact tuff.

4.2.1 Solubility-Limited Release Directly into Tuff

Here we conservatively assume that the tuff is in direct contact with bare waste. In Figure 7 we show the release rates of Np-237, Am -241, Am-243, U-234 and U-238 from spent fuel and borosilicate glass, normalized to the 1000-year inventories and plotted against time since first water contact. Eq. (61) in Sadeghi *et al.*[1] is used for this calculation of solubility-limited diffusive release into water in the surrounding rock. Constant isotopic compostion of each elemental species in the undissolved waste is assumed. In all cases the fractional release rates start out high. The fractional release rates of U-234 and U-238 coincide. For each of the species the calculated release rate terminate where decay in the undissolved waste would result in a large overestimate from the equations used to calculate release rate.

Figure 8 shows the normalized release rates of plutonium isotopes from spent fuel and borosilicate glass.

The differences between the fractional release rates for spent fuel and glass are due to the differences in solubilities and inventories used in the calculations as discussed in Section 4.1. All release rates are much greater than those for the wet-drip water-contact mode.

4.2.2 Solubility-Limited Release Through a Rubble-Filled Annulus

Here we assume a failed waste container in physical contact with sediments or exfoliated tuff in the annulus between the container and intact rock. The annulus is surrounded by intact tuff. We refer to the material in the annulus as rubble and assume that each rubble piece has the same moisture content as the surrounding tuff.

To calculate the diffusive release rates for solubility-limited species under these conditions, eq. (76) from Sadeghi *et al.*[1] is used. Two important parameters in (76) are the diffusion coefficient and the effective porosity.

The diffusion coefficient for radionuclides in a water continuum, 1×10^{-5} cm^2/s, has been previously used in conservative release calculations for waste packages emplaced in tuff.[2,6] When used for calculating diffusion through porous media, this value conservatively ignores tortuosity effect and diffusion reduction due to unconnected water-filled pores in the rock matrix.

For transport through an unconsolidated rubble bed of partially saturated porous rock, there are additional tortuosity effects. Under the partial-saturation conditions expected at the emplacement horizon at Yucca Mountain, no water films are expected on the surfaces of rubble pieces. Transport is constrained to diffusion through interconnected water-filled pores within rubble pieces, through areas of contact between adjacent rubble pieces, through contact areas between rubble pieces and intact rock, and through contact areas between rubble pieces and the surface of the degraded waste container. Diffusion through pore liquid in contacting rubble pieces and through contact areas has received preliminary examination by experiments and by theoretical analysis for diffusional transport through beds of tuff gravel.[21,22] Both studies show that for the degree of partial saturation assumed for the Yucca Mountain site, the effective diffusion coefficient through gravel-sized rubble pieces is likely to be many orders of magnitude below that of intact rock. A thousand-fold reduction below that of intact rock is adopted for this study.

In calculating the Fick's-law diffusive flux (g/cm^2-s) through pore liquid in unsaturated intact rock, the effective porosity that appears in the flux boundary condition at an interface is the product of the rock-matrix porosity ϵ_r and the saturation fraction Ψ, i.e., the fraction of the pores that are water filled. This assumes isotropic porosity and continuous diffusive pathways through water-filled pores. The $\epsilon_r\Psi$ product is defined as the liquid transport porosity ϵ_t for intact rock and is used wherever the porosity appears in equations derived for mass transport through an equivalent saturated porous medium. It neglects the fracture porosity of intact rock, only a small correction for unsaturated tuff.

To calculate the sorption retardation coefficient for transport in unsaturated porous rock, assuming local chemical equilibrium between a species in the pore liquid and that same species sorbed in the rock, the retardation coefficient K is given by

$$K = 1 + \frac{1-\epsilon_r}{\epsilon_r \Psi} K_d \tag{1}$$

where K_d is the dimensionless distribution coefficient (mass per unit volume of rock solid divided by mass per unit volume of pore liquid)
ϵ_r is the overall porosity of the rock matrix
Ψ is the fractional saturation of the rock matrix.

For a gravel bed of unsaturated rock pieces, we define ϵ_b as the rubble-bed porosity, i.e., the volume of air between rubble pieces divided by the total bed volume. Here the effective porosity ϵ_t that appears in the flux boundary condition at an interface, and that appears explicitly in the transport equations for an equivalent saturated porous medium, is approximated by

$$\epsilon_t = (1-\epsilon_b)\epsilon_r \Psi \tag{2}$$

For the porosity and saturation values in Table IX, the effective porosity for transport is 0.096.

Figure 9 shows the normalized release rates of plutonium isotopes from spent fuel and glass into intact tuff, for water-continuum diffusion coefficient in the annulus and also for a 1000-fold reduction in the annulus diffusion coefficient. Using the water-continuum diffusion coefficient, the plutonium species would arrive at the emplacement borehole wall in about 20 years. However, if the annulus is unsaturated and filled with rubble, with the annulus diffusion coefficient reduced 1000-fold, plutonium would arrive at the borehole wall after about 30,000 years. Comparing Figure 9 with Figure 8, the presence of an unsaturated annulus eliminates the high fractional release rates at early times.

With the 1000-fold reduction in the annulus diffusion coefficient, Pu-242 has the highest release rate into the surrounding rock. During the 30,000 years for plutonium to diffuse through the annulus with the reduced diffusion coefficient, most of the Pu-240 and Pu-239 will have decayed. Another benefit of the reduced diffusion coefficient is the much lower peak fractional release rates.

Figure 10 shows the fractional release rates of neptunium from spent fuel and glass, for a water-continuum annulus diffusion coefficient and for a 1000-fold reduction in diffusion coefficient. Using the water-continuum diffusion coefficient, Np-237 would arrive at the emplacement hole wall in less than a year, because of its relatively low retardation coefficient. For a 1000-fold reduction in diffusion coefficient Np-237 would arrive after 1,000 years, with a 1000-fold reduction in the peak fractional release rate.

4.2.3 Alteration-Controlled Release Through a Rubble-Filled Annulus

Here we consider the release of Tc-99, I-129 and Cs-135 from spent fuel and Tc-99 and Cs-135 from borosilicate glass when the release is controlled by the alteration of UO_2 to U_3O_8. These species also have instant release fractions, but we showed in Figure 6 that the alteration of the fuel matrix dominates the release rate of soluble species. Thus we consider here only the alteration-controlled release. Figure 11 shows the alteration-controlled release rates of Tc-99, I-129 and Cs-135 from spent fuel and Tc-99 and Cs-135 from borosilicate glass, with a 1000-fold reduction in diffusion coefficient in the unsaturated rubble-filled annulus. I-129 from spent fuel is the first to arrive at the emplacement borehole wall, and its fractional release rate reaches a maximum at about 1,000 years, but below its repository-average limit of 5×10^{-4} per year. I-129 is a low-inventory species and its release rate limit is 10^{-8} of the total curies inventory of the entire repository at 1000 years.

Tc-99, with marginal retardation, arrives shortly thereafter, and also reaches its peak fractional release rate at about 1000 years. For bare spent fuel in the moist-continuous water-contact mode, the single-package fractional release rates of Tc-99 and I-129 are above the repository-average limit of 1×10^{-5} per year, and consideration must be given to the effect of the partly intact container and to the time distribution of container failures.

Strongly sorbing Cs-135 does not reach the borehole wall until 10,000 years after water contact. Its peak

fractional release rate is below its low-inventory limit of 5 $\times 10^{-5}$ per year.

Releases from borosilicate glass show arrival times identical with those for spent fuel. Because of the lower alteration rate in glass, the peak fractional release rates are lower and the peaks occur later than for spent fuel.

5. CONCLUSIONS AND RECOMMENDATIONS

We have calculated release rates for key radionuclides from spent fuel and borosilicate glass from the engineered barrier system of a potential nuclear waste repository in unsaturated tuff. These radionuclides have been selected because of their high inventory, low retardation in the geosphere, and long half life, and thus are important radionuclides to study in safety assessment of nuclear waste repositories.

The calculated release rates are for both the wet-drip bathtub and the moist-continuous water-contact modes. These release rates are primarily to illustrate the method of analysis, and the numerical results reflect the quality of input data.

The release rates of actinides are controlled primarily by their elemental solubilities. The peak release rates of most actinides are well below the USNRC limit for annual release rates.

For fission product species, the release rates are dominated by the solid-solid alteration process in the waste matrix. The instant dissolution fractions, present in the fuel-cladding gap, fuel plenum and grain boundaries in about one to two percent, do not significantly affect the release rates in either water contact mode. The peak release rates of Cs-135, I-129 and Tc-99 are in the same order of magnitude for the two water contact modes.

These are the most important parameters which require measurements to validate the calculated release rates:

Water Infiltration Rate

In the wet-drip water-contact mode, the water infiltration rate determines the beginning and duration of water contact and the beginning of release. For low-solubility species it determines the rate of release. It is therefore an important parameter. The moist-continuous water-contact mode requires only interconnecting pore-water. Except for very large changes in water infiltration rates, the moist-continuous release rates are not sensitive to the water infiltration rate.

Solubility

In Section 3.3 we discussed at length the uncertainties associated with solubilities for calculating release rates. Improved estimates of actinide solubilites will improve the reliability of calculated release rates.

Alteration Rate

The release rates of the fission products Cs-135, I-129, and Tc-99 are controlled by matrix alteration and corrosion. At present we must rely on empirical data on the alteration rate of spent fuel and the corrosion rate of glass to predict the release rates of these soluble fission products. Improved understanding of spent-fuel matrix alteration and glass corrosion, as well as more extensive laboratory data, will improve the reliability of release-rate calculations for these species.

Diffusion Coefficient

In the moist-continuous water-contact mode, mass transfer rate depends strongly on the diffusion coefficients in the rubble and in intact rock. Both theory and measurements have shown that the effective diffusion coefficient in an unsaturated rubble-filled annulus can be several orders of magnitude below that of intact rock. Improved measurements of the effective diffusion coefficients are needed. The theoretical analysis of the effective diffusion coefficient in a rubble-filled annulus identifies the parameters that will effect the measurement and that should be considered in planning experiments.

In all the above data needs, all except water infiltration rate can be determined from laboratory studies.

Water-contact Mode

More realistic analyses of water-contact modes are needed. The extent to which ground water drips onto the container, the extent to which the drips penetrate a failed container, and the extent to which radionuclides dissolved in container water leak or diffuse out of container penetrations are uncertainties in the wet-drip mode. A detailed analysis of evaporation of drips and diffusion of water vapor into surrounding unsaturated rock is now underway and is expected to yield better insight into the fate of ground water dripping onto a container.

It is conservative but unrealistic to assume that in the moist-continuous mode the failed container offers no barrier to mass transfer of dissolved radionuclides from within the container into the surrounding rock or rubble. A detailed analysis that takes into account the mass-transfer resistance of penetrations in a failed container is underway.

These new analyses can lead to a more realistic predictive technique that unifies the wet-drip and moist-continuous water-contact modes.

REFERENCES

1. M. M. Sadeghi, T. H. Pigford, P. L. Chambré and W. W.-L. Lee, "Equations for Predicting Release Rates for Waste Packages in Unsaturated Tuff," LBL-29254, 1990.

2. T. H. Pigford and W. W.-L. Lee, "Waste Package Performance in Unsaturated Rock," Proceedings of FOCUS '89, Nuclear Waste Isolation in the Unsaturated Zone, 145, 1989.

3. T. H. Pigford, P. L. Chambré and W. W.-L. Lee, *A Review of Near-Field Mass Transfer in Geologic Disposal Systems,* LBL-27045, 1989.

4. U.S. Department of Energy, "Characteristics of Spent Fuel, High-Level Waste, and Other Radioactive Wastes Which May Require Long-Term Isolation," DOE/RW-0184, 1987.

5. U.S. Department of Energy, "Site Characterization Plan, Yucca Mountain Site, Nevada Research and Developement Area, Nevada," DOE/RW-0199, 1988.

6. M. J. Apted, W. J. O'Connell, K. H. Lee, A. T. MacIntyre, T.-S. Ueng, T. H. Pigford and W. W.-L. Lee, "Preliminary Calculations of Release Rates of Tc-99, I-129, Cs-135, & Np-237 from Spent Fuel in a Tuff Repository," WG2-5-90, 1990.

7. R. S. Rundberg, "Assessment Report on the Kinetics of Radionuclide Adsorption on Yucca Mountain Tuff," LA-11026-MS, 1987.

8. M. M. Sadeghi, W. W.-L. Lee, T. H. Pigford and P. L. Chambré, "Diffusive Release of Radionuclides into Saturated and Unsaturated Tuff," *Trans. Am. Nuc. Soc., 61,* 70, 1990.

9. M.J. Nicol and C.R.S. Needes, "The Anodic Dissolution of Uranium Dioxide–I. in Perchlorate Solutions," *Electrochim. Acta, 20,* 585, 1975; "The Anodic Dissolution of Uranium Dioxide–II. in Carbonate Solutions," *Electrochim. Acta, 22,* 1381, 1977.

10. D.W. Shoesmith, S. Sunder, M.G. Bailey and G.J. Wallace, "Anodic Oxidation of UO_2. Electrochemical and X-ray photoelectron spectroscopic studies of film-growth and dissolution in phosphate-containing solutions," *Can. J. Chem. 66,* 259, 1988.

11. L.H. Johnson and D.W. Shoesmith, "Spent Fuel," in W. Lutze and R.C. Ewing (eds.), *Radioactive Waste Forms for the Future,* Amsterdam: Elsevier, 1988.

12. C. N. Wilson, "Results from NNWSI Series 3 Spent Fuel Dissolution Tests," PNL-7170, 1990.

13. T. A. Abrajano, J. K. Bates, T. J. Gerding, and W. L. Ebert, "The Reaction of Glass During Gamma Irradiation in a Saturated Tuff Environment, Part III: Long Term Experiments at 10^4 rad/hr," ANL-88-14, 1988.

14. C. N. Wilson and C. J. Bruton, "Studies on Spent Fuel Dissolution Behavior under Yucca Mountain Repository Conditions," PNL-SA-16832, 1989.

15. C.J. Bruton, "Geochemical Simulation of Dissolution of West Valley and DWPF Glasses in J-13 Water

at 90°C." in *Scientific Basis for Nuclear Waste Management XI*, eds. M.J. Apted and R.E. Westerman, Materials Research Society, Pittsburgh, PA, 607, 1988.

16. C. J. Bruton and H. Shaw, "Geochemical Simulation of Reaction between Spent Fuel Waste Form and J-13 Water at 25°C and 90°C, " in *Scientific Basis for Nuclear Waste Management XI*, eds. M.J. Apted and R.E. Westerman, Materials Research Society, Pittsburgh, PA, 485, 1988.

17. H. Nitsche, "Basic Research for Assessment of Geologic Nuclear Waste Repositories: What Solubility and Speciation Studies of Transuranium Elements Can Tell Us," to appear in in *Scientific Basis for Nuclear Waste Management XIV*, eds. T. A. Abrajano and L. H. Johnson, Materials Research Society, Pittsburgh, PA, 1991.

18. J. A. Rard, "Critical Review of the Chemistry and Thermodynamics of Technetium and Some of its Inorganic Compounds and Aqueous Species," UCRL-53440, 1983.

19. K. O. Bennington, R. P. Beyer and G. K. Johnson, "Thermodynamics Properties of Pollucite," Bureau of Mines Report of Investigations 8779, 1983.

20. C. L. Kim, P. L. Chambré and T. H. Pigford, "Radionuclide Release Rates as Affected by Container Failure Probability," *Trans. Am. Nuc. Soc., 50,* 136, 1985.

21. J. Conca, "Diffusion Barrier Transport Properties of Unsaturated Paintbrush Tuff Rubble Backfill," Proc. of the International High-Level Waste Management Conference, Las Vegas, 394, 1990.

22. M. M. Sadeghi, W. W.-L. Lee, T. H. Pigford & P. L. Chambré, "The Effective Diffusion Coefficient for Porous Rubble," *Trans. Am. Nuc. Soc., 61,* 67, 1990.

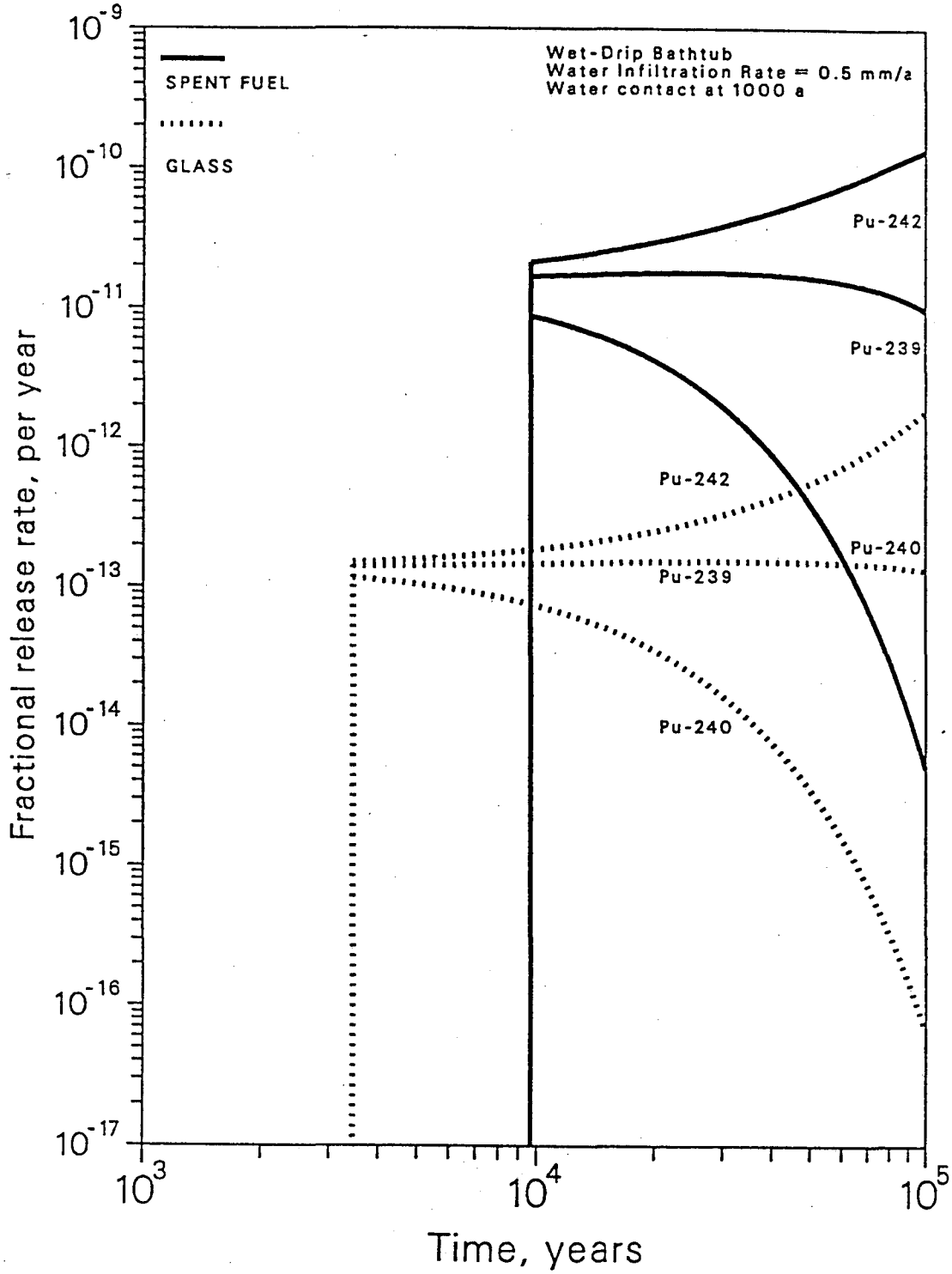

Fig. 2. Fractional release rates of plutonium isotopes, wet-drip bathtub, water contact at 1000 years, water infiltration rate 0.5 mm/a

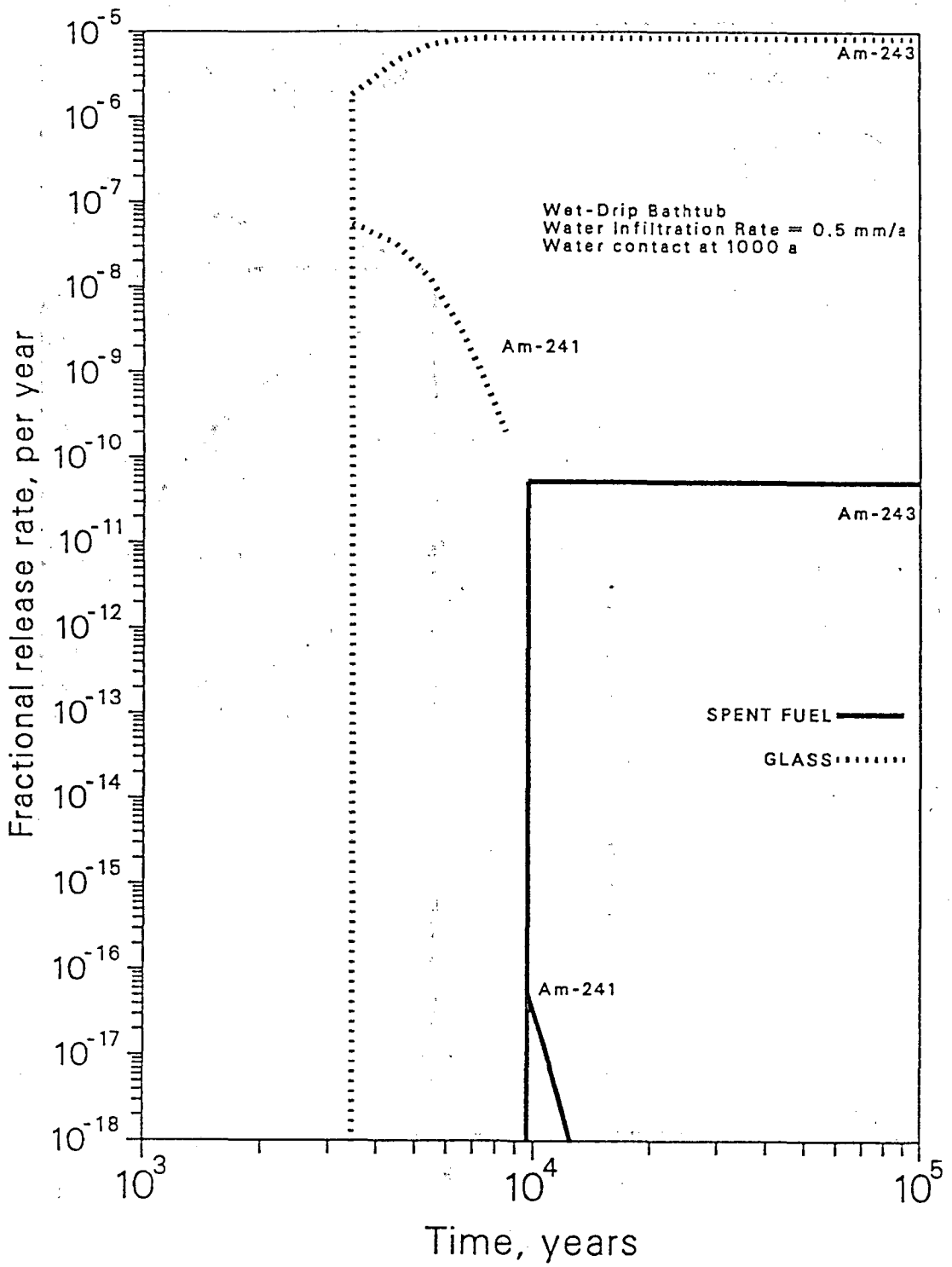

Fig. 3. Fractional release rates of americium isotopes, wet-drip bathtub, water contact at 1000 years, water infiltration rate 0.5 mm/a

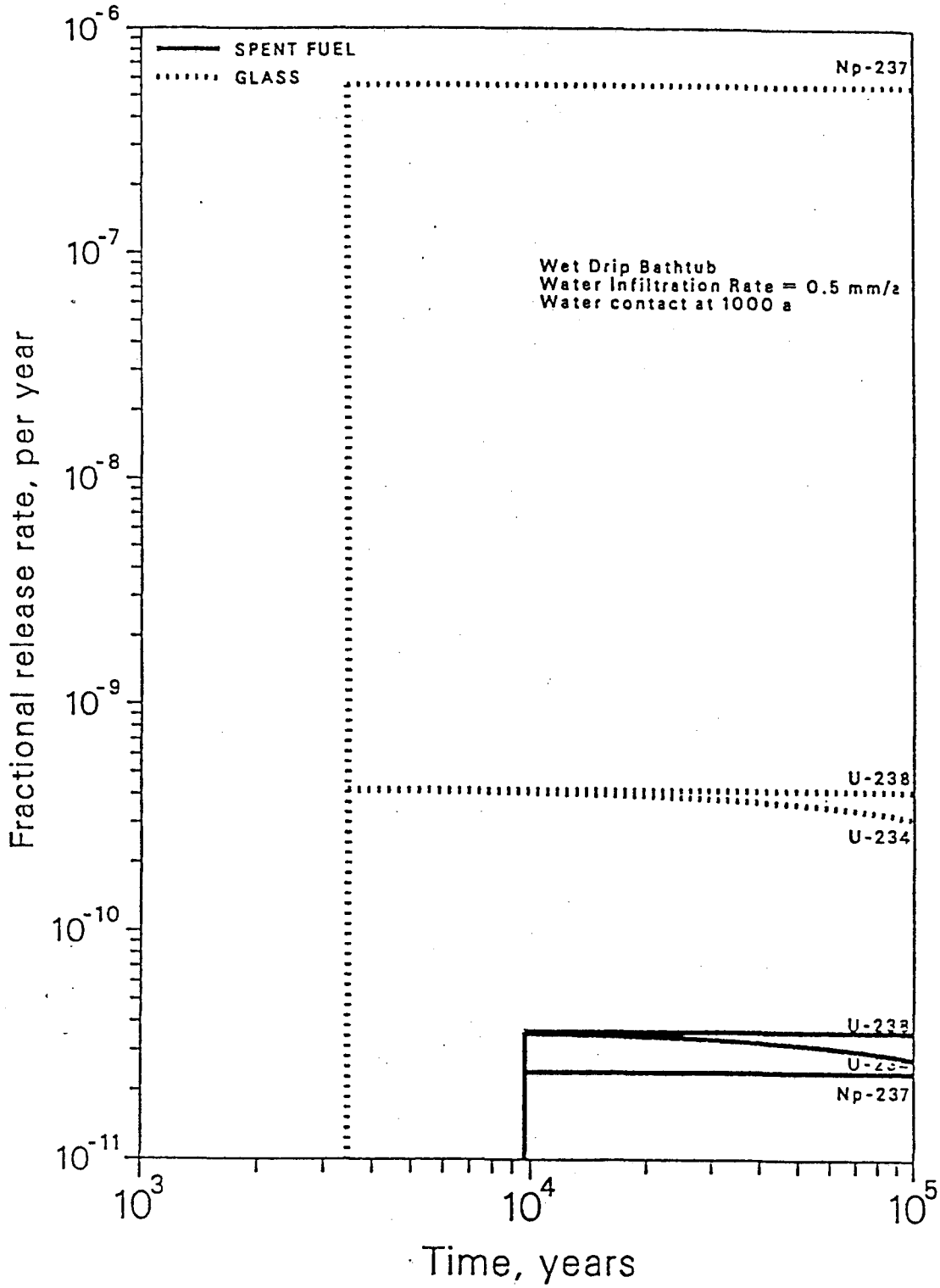

Fig. 4. Fractional release rates of neptunium and uranium isotopes, wet-drip bathtub, water contact at 1000 years, water infiltration rate 0.5 mm/a

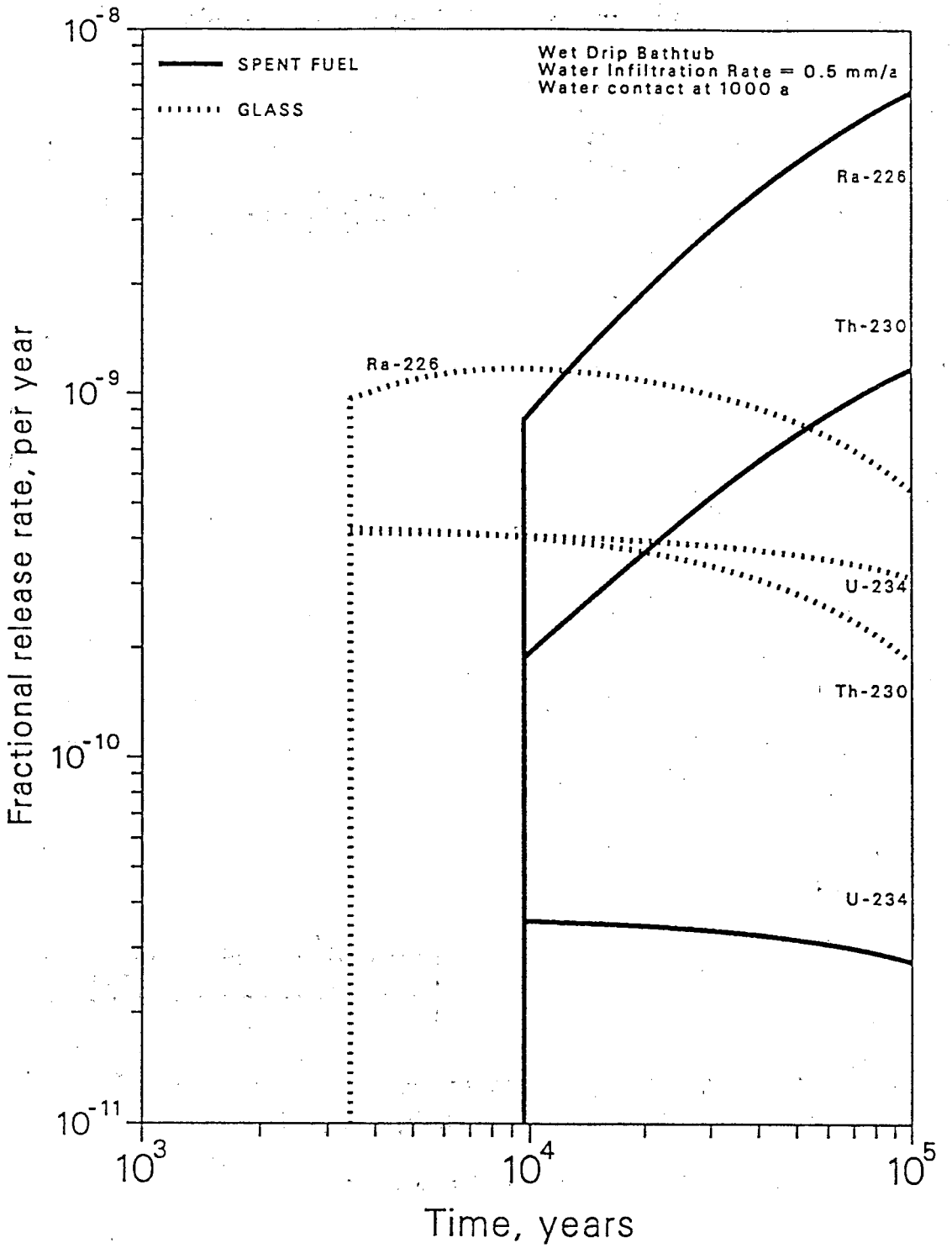

Fig. 5. Fractional release rates of U-234→Th-230→Ra-226 chain, wet-drip bathtub, water contact at 1000 years, water infiltration rate 0.5 mm/a

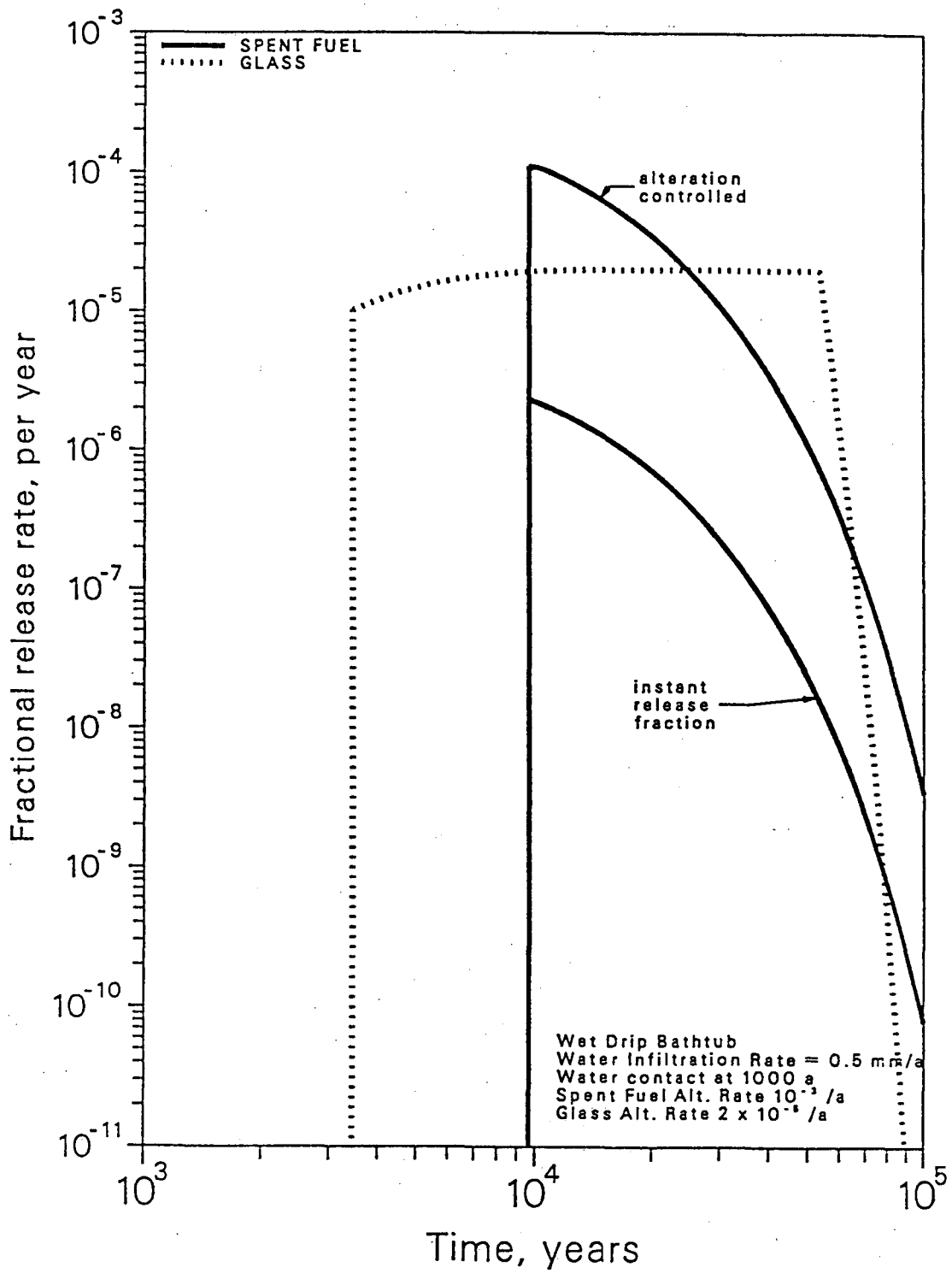

Fig. 6. Fractional release rates of alteration-controlled species and their instant release fractions, wet-drip bathtub, water contact at 1000 years, water infiltration rate 0.5 mm/a

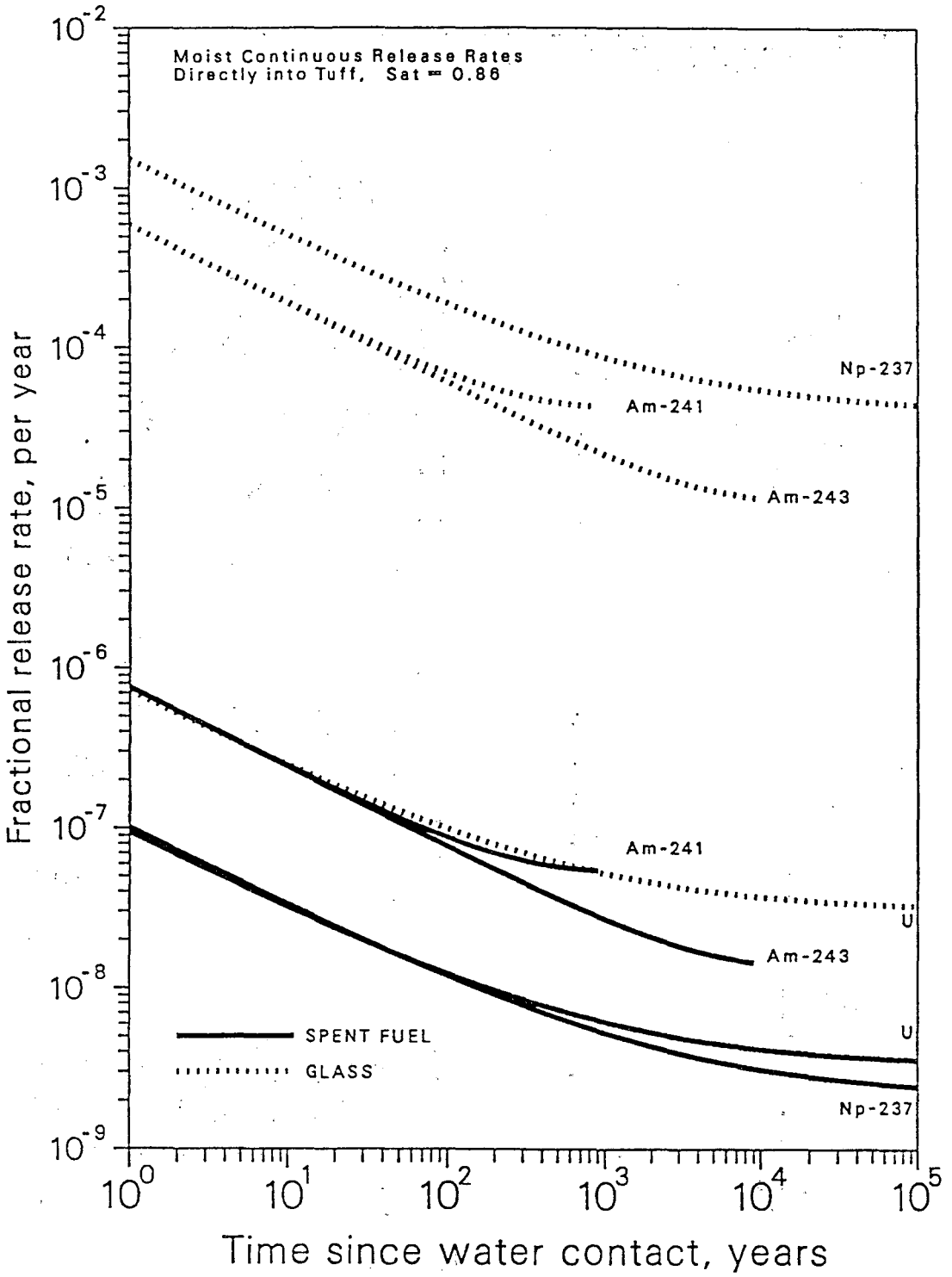

Fig. 7. Fractional release rates of americium, neptunium and uranium isotopes directly into intact tuff, moist-continuous water contact

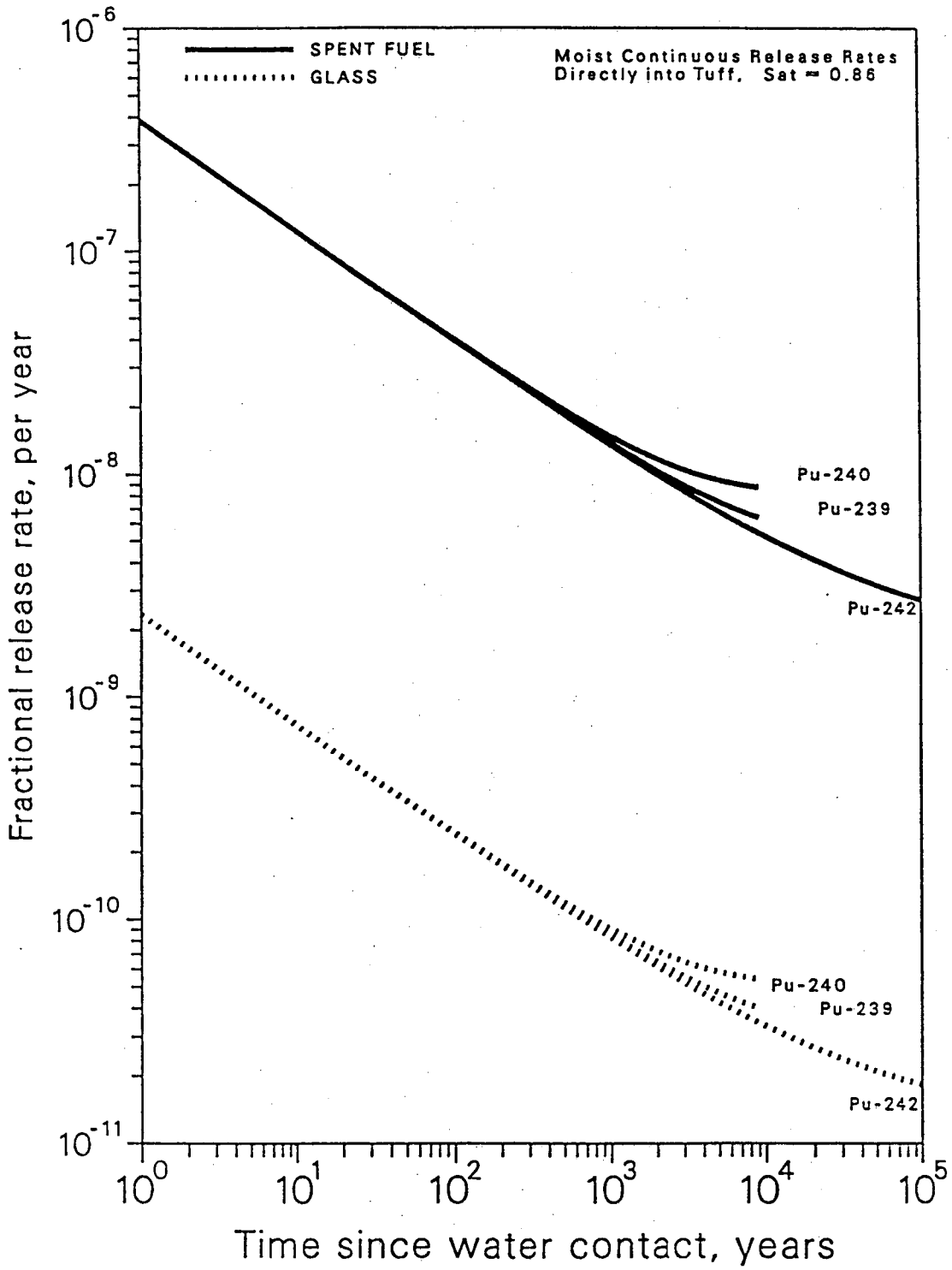

Fig. 8. Fractional release rates of plutonium isotopes directly into intact tuff, moist-continuous water contact.

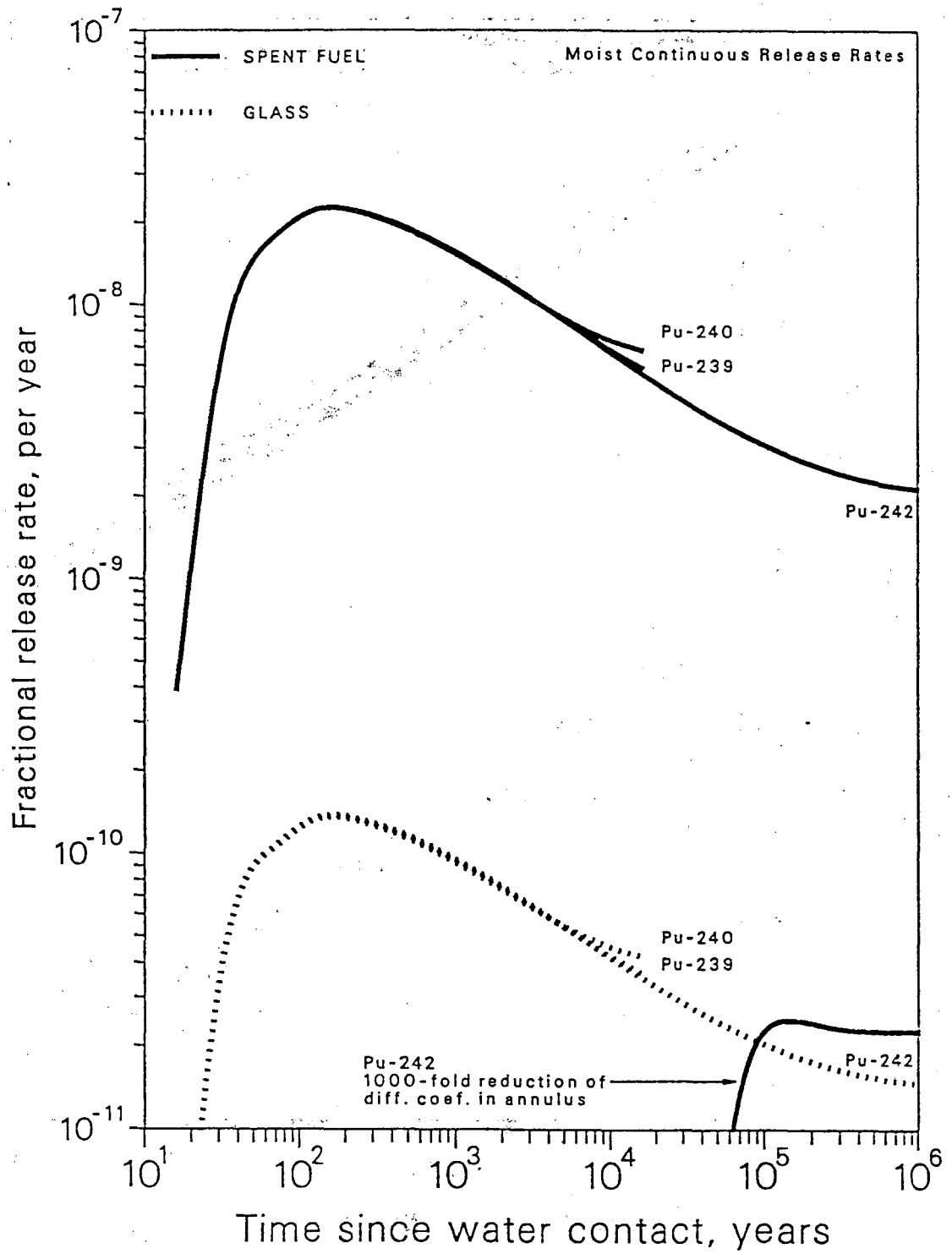

Fig. 9. Fractional release rates of plutonium isotopes through a rubble-filled annulus into intact tuff, moist-continuous water contact, with 1000-fold reduction of diffusion coefficient in annulus

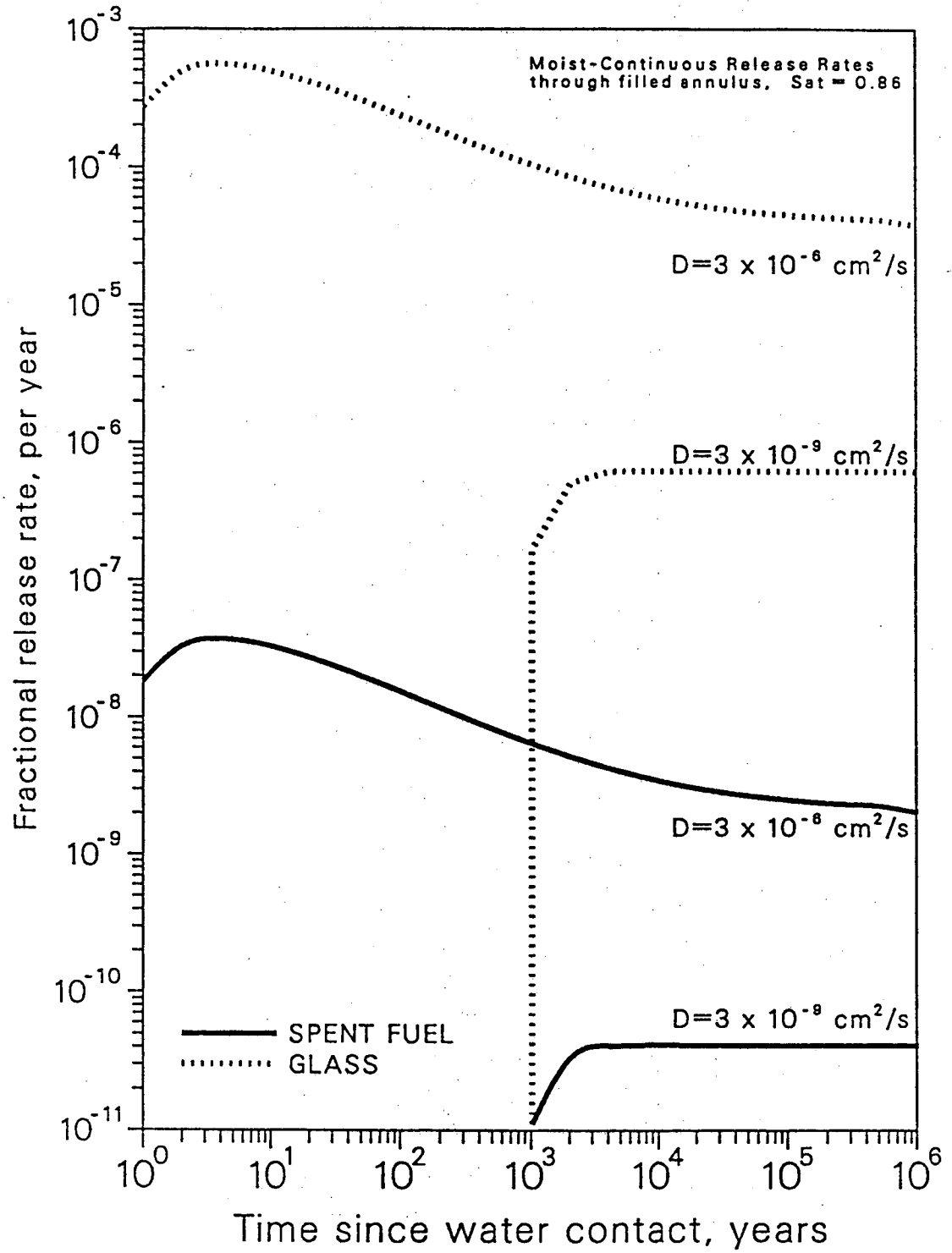

Fig. 10. Fractional release rates of americium isotopes through a rubble-filled annulus into intact tuff, moist-continuous water contact, with 1000-fold reduction of diffusion coefficient

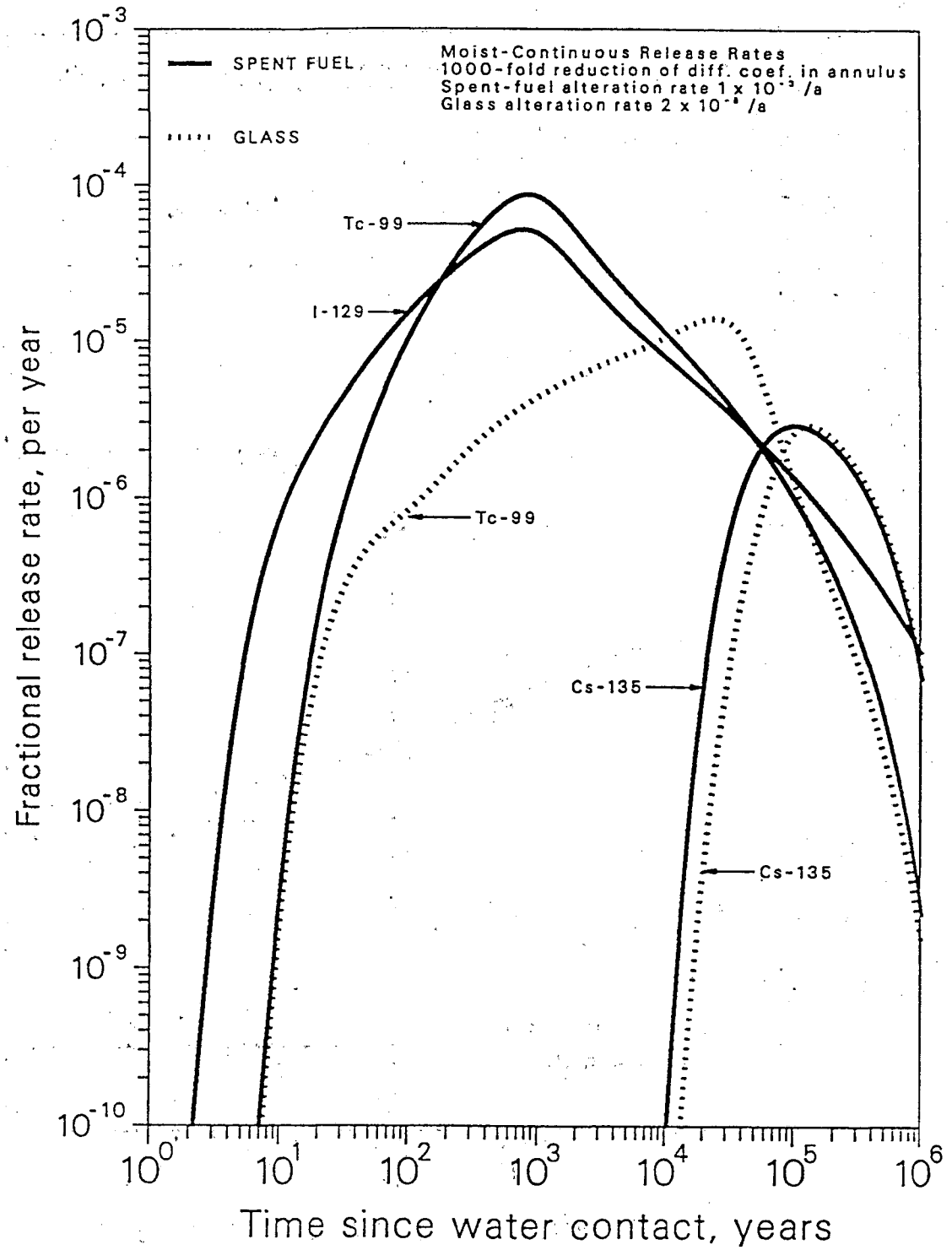

Fig. 11. Fractional release rates of alteration-controlled species, through a rubble-filled annulus into intact tuff, moist-continuous water contact, with 1000-fold reduction of diffusion coefficient in annulus

LAWRENCE BERKELEY LABORATORY
UNIVERSITY OF CALIFORNIA
INFORMATION RESOURCES DEPARTMENT
BERKELEY, CALIFORNIA 94720